Article

Assembly of a Homochiral, Body-Centered Cubic Network Composed of Vertex-Shared Mg Cages: Use of Electrospray Ionization Mass Spectrometry to Monitor Metal Carboxylate Nucleation

Jeffrey A. Rood, William C. Boggess, Bruce C. Noll, and Kenneth W. Henderson

J. Am. Chem. Soc., **2007**, 129 (44), 13675-13682• DOI: 10.1021/ja074558j • Publication Date (Web): 10 October 2007

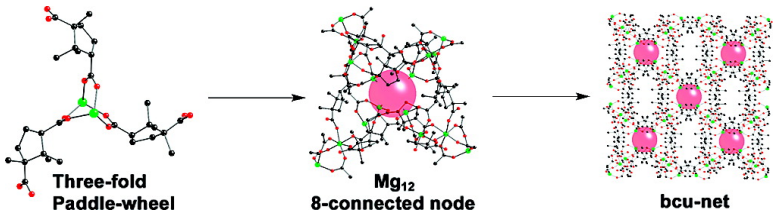

More About This Article

Additional resources and features associated with this article are available within the HTML version:

- Supporting Information
- Links to the 12 articles that cite this article, as of the time of this article download
- Access to high resolution figures
- Links to articles and content related to this article
- Copyright permission to reproduce figures and/or text from this article

View the Full Text HTML

J|A|C|S
ARTICLES
Published on Web 10/10/2007

Assembly of a Homochiral, Body-Centered Cubic Network Composed of Vertex-Shared Mg_{12} Cages: Use of Electrospray Ionization Mass Spectrometry to Monitor Metal Carboxylate Nucleation

Jeffrey A. Rood, William C. Boggess, Bruce C. Noll, and Kenneth W. Henderson*

Contribution from the Department of Chemistry and Biochemistry, University of Notre Dame, Notre Dame, Indiana 46556-5670

Received June 21, 2007; E-mail: khenders@nd.edu

Abstract: Reaction of $Mg(NO_3)_2 \cdot 6H_2O$ with (+)-camphoric acid (H_2cam) in acetonitrile results in the immediate formation of soluble, dimetallic $[Mg_2(Hcam)_3]^+$ cations. The formation of these stable cations in solution was determined by electrospray ionization mass spectrometry (ESI−MS). These dimers are 3-fold paddle-wheels, which associate together through the neutral acid units to build the metal-organic framework $[Mg_2(Hcam)_3 \cdot 3H_2O] \cdot NO_3 \cdot MeCN$, **1**. The network consists of a series of fused Mg_{12} cages that have 12 water molecules at their centers, creating isolated 0D cavities within the structure. Overall, the extended structure of **1** is a body-centered cubic (**bcu**) lattice, with the Mg_{12} cages being utilized as eight-connected nodes. The framework of **1** is chiral and adopts the very unusual space group *I*23. Use of 1,3-propanediol as an additive results in the formation of the simple 1D polymer $[Mg(cam)\{HO(CH_2)_3OH\}_2]$, **2**. In **2**, each carboxylate-bridged metal center is chelated by two diols. ESI−MS studies confirm the formation of new ions in these solutions. The identities of **1** and **2** were confirmed by a combination of single-crystal X-ray diffraction, elemental analyses, IR, NMR, themogravimetric analyses, and ESI−MS data. ESI−MS has proven to be a valuable technique in the identification of stable SBUs in solution prior to network formation.

Introduction

Metal-organic frameworks (MOFs) have received considerable attention due to their potential applications[1] in areas such as catalysis,[2] optics,[3] electronics,[4] small molecule storage,[5] and separation science.[6] A popular strategy for the synthesis of these networks has been through the combination of transition metal salts with ditopic carboxylate ligands.[7] In comparison, relatively little attention has been given to the use of s-block metals in the construction of MOFs.[8] However, the use of such metals in porous materials is appealing as they are predicted to have strong binding affinities for some small molecules such as dihydrogen,[9] making them candidates as lightweight sorption materials.[10] Furthermore, considering the widespread use of s-block metal

(1) (a) Mueller, U.; Schubert, M.; Teich, F.; Puetter, H.; Schierle-Arndt, K.; Pastre, J. *J. Mater. Chem.* **2006**, *16*, 626. (b) Champness, N. R. *Dalton Trans.* **2006**, 877. (c) Champness, N. R.; Schröder, M. *Curr. Opin. Solid State Mater.* **1998**, *3*, 419. (d) Janiak, C. *Dalton Trans.* **2003**, 2781. (e) Papaefstathiou, G. S.; MacGillivray, L. R. *Coord. Chem. Rev.* **2003**, *246*, 169. (f) Braga, D. *Chem. Commun.* **2003**, 2751. (g) James, S. L. *Chem. Soc. Rev.* **2003**, *32*, 276. (h) Batten, S. R. *Curr. Opin. Solid State Mater.* **2001**, *5*, 107. (i) Zaworotko, M. J. *Chem. Commun.* **2001**, 1. (j) Braga, D. *J. Chem. Soc. Dalton Trans.* **2000**, 3705. (k) Zaworotko, M. J. *Angew. Chem. Int. Ed.* **2000**, *39*, 3052.

(2) (a) Wu, C.; Hu, A.; Zhang, L.; Lin, W. *J. Am. Chem. Soc.* **2005**, *127*, 8940. (b) Perles, J.; Iglesias, M.; Martin-Luengo, M.; Monge, M. A.; Ruiz-Valero, C.; Snejko, N. *Chem. Mater.* **2005**, *17*, 5837. (c) Uemara, T.; Kitagawa, K.; Horike, S.; Kawamura, T.; Kitagawa, S. *Chem.Commun.* **2005**, 5968. (d) Schlichte, K.; Kratzke, T.; Kaskel, S. *Micropor. Mesopor. Mater.* **2004**, *73*, 81. (e) Seo, J. S.; Whang, D.; Lee, H.; Jun, S. I.; Oh, J.; Jeon, Y.; Kim, K. *Nature*. **2000**, *404*, 982. (f) Fujita, M.; Kwon, Y. J.; Washizu, S.; Ogura, K. J. *J. Am. Chem. Soc.* **1994**, *116*, 1151.

(3) (a) Zhang, L.; Yu, J.; Xu, J.; Lu, J.; Bie, H.; Zhang, X. *Inorg. Chem. Commun.* **2005**, *8*, 638. (b) Zhao, B.; Chen, X. Y.; Cheng, P.; Liao, D. Z.; Yan, S. P.; Jiang, Z. H. *J. Am. Chem Soc.* **2004**, *126*, 15394.

(4) (a) Wang, L.; Yang, M.; Shi, Z.; Chen, Y.; Feng, J. *J. Solid State Chem.* **2005**, *178*, 3359. (b) Dietzel, P. D. C.; Morita, Y.; Blom, R.; Fjellvaag, H. *Angew. Chem., Int. Ed.* **2005**, *44*, 6354. (c) Poulsen, R. D.; Bentien, A.; Chevalier, M.; Iversen, B. B. *J. Am. Chem. Soc.* **2005**, *127*, 9156. (d) Cui, H.; Takahashi, K.; Okano, Y.; Kobayashi, H.; Wang, Z.; Kobayashi, A. *Angew. Chem., Int. Ed.* **2005**, *44*, 6508.

(5) (a) Lee, Y. J.; Li, J.; Jagiello, J. *J. Solid State Chem.* **2005**, *178*, 2527. (b) Wang, Q. M.; Shen, D. M.; Bulow, M.; Lau, M. L.; Deng, S. G.; Fitch, F. R.; Lemcoff, N. O.; Semanscin, J. *Micropor. Mesopor. Mater.* **2002**, *55*, 217. (c) Fletcher, A. J.; Cussen, E. J.; Prior, T. J.; Rosseinsky, M. J. *J. Am. Chem. Soc.* **2001**, *123*, 10001.

(6) (a) Chen, B.; Liang, C.; Yang, J.; Contreras, D. S.; Clancy, Y. L.; Lobkovsky, E. B.; Yaghi, O. M.; Dai, S. *Angew. Chem., Int. Ed.* **2006**, *45*, 1390. (b) Choi, H. J.; Suh, M. P. *J. Am. Chem. Soc.* **2004**, *126*, 15844. (c) Ohmori, O.; Kawano, M.; Fujita, M. *J. Am. Chem. Soc.* **2004**, *126*, 16292. (d) Dybtsev, D. N.; Chun, H.; Kim, K. *Angew. Chem., Int. Ed.* **2004**, *43*, 5033; (e) Lu, J. Y.; Babb, A. M. *Chem. Commun.* **2002**, 1340.

(7) (a) Roswell, J. L. C.; Yaghi, O. M. *Angew. Chem., Int. Ed.* **2005**, *44*, 4670. (b) Rosi, N. L.; Kim, J.; Eddaoudi, M.; Chen, B.; O'Keeffe, M.; Yaghi, O. M. *J. Am. Chem. Soc.* **2005**, *127*, 1504. (c) Yaghi, O. M.; O'Keeffe, M.; Ockwig, N.; Chae, H. K.; Eddaoudi, M.; Kim, J. *Nature*. **2003**, *423*, 705. (d) Eddaoudi, M.; Moler, D.; Li, H.; Reinke, T. M.; O'Keeffe, M.; Yaghi, O. M. *Acc. Chem. Res.* **2001**, *34*, 319. (e) Kim, J.; Chen, B.; Reinke, T. M.; Li, H.; Eddaoudi, M.; Moler, D. B.; O'Keeffe, M.; Yaghi, O. M. *J. Am. Chem. Soc.* **2001**, *123*, 8239. (f) O'Keeffe, M.; Eddaoudi, M.; Li, H.; Reinke, T. M.; Yaghi, O. M. *J. Solid State Chem.* **2000**, *152*, 3. (g) Reinke, T. M.; Eddaoudi, M.; O'Keeffe, M.; Yaghi, O. M. *Angew. Chem., Int. Ed.* **1999**, *38*, 2590. (h) Eddaoudi, M.; Li, H.; Reinke, T. M.; Fehr, M.; Kelley, D.; Groy, T. L.; Yaghi, O. M. *Top. Catal.* **1999**, *9*, 105.

(8) (a) Morris, J. J.; Noll, B. C.; Henderson, K. W. *Cryst. Growth Des.* **2006**, *6*, 1071. (b) MacDougall, D. J.; Noll, B. C.; Kennedy, A. R.; Henderson, K. W. *Dalton Trans.* **2006**, 1875. (c) MacDougall, D. J.; Kennedy, A. R.; Noll, B. C.; Henderson, K. W. *Dalton Trans.* **2005**, 2084. (d) MacDougall, D. J.; Morris, J. J.; Noll, B. C.; Henderson, K. W. *Chem. Commun.* **2005**, 456. (e) MacDougall, D. J.; Noll, B. C.; Henderson, K. W. *Inorg. Chem.* **2005**, *44*, 1181. (f) Henderson, K. W.; Kennedy, A. R.; Macdonald, L.; MacDougall, D. J. *Inorg. Chem.* **2003**, *42*, 2839. (g) Henderson, K. W.; Kennedy, A. R.; MacDougall, D. J.; Shanks, D. *Organometallics* **2002**, *21*, 606.

(9) Lochan, R. C.; Head-Gordon, M. *Phys. Chem. Chem. Phys.* **2006**, *8*, 1357.

complexes in both organic and inorganic synthesis,[11] the preparation of porous solids incorporating these elements opens up the opportunity to create solid-state reagents. Recently, we and others have prepared the first examples of permanently porous magnesium carboxylate frameworks.[12,13] These materials have proven to be more thermally robust than their transition metal analogues and have been shown to be useful in the molecular exchange of small molecules and also in the sorption of various gases including dihydrogen. We have sought to extend our work in this area toward the formation of homochiral frameworks for use in enantioselective separations and heterogeneous asymmetric syntheses.[14−22] We chose to investigate the use of (+)-camphoric acid (H_2cam = camphoric acid) as an enantiopure ditopic organic linker as it is commercially available, relatively inexpensive and is unlikely to undergo racemization.[23] The configurational stability of camphoric acid is due to racemization requiring the cleavage of strong C−C bonds. In comparison, most readily available chiral pool acids can readily undergo epimerization at their enantiomeric centers under the conditions used for network formation (Figure 1).[14−22]

During the present study, we also chose to address one of the central questions in MOF chemistry: the mechanism of self-assembly from soluble solution species to extended solid-state materials.[24] Although there has been a great deal of interest in classifying MOF structures and attempting to build some level of predictability into the design of extended networks,[25]

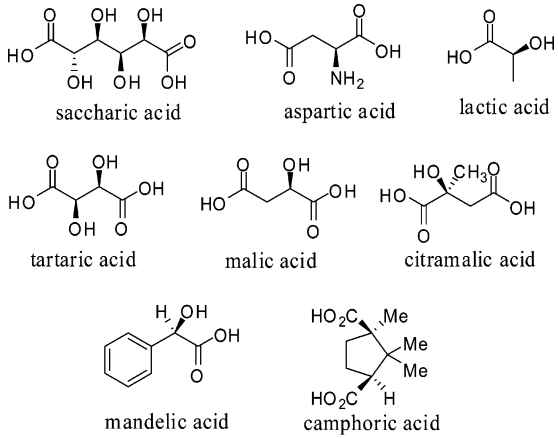

Figure 1. Selection of chiral pool acids used to prepare metal−organic frameworks.

relatively little focus has been directed toward analyzing the synthons in solution that are precursors for building the solids. In part, this is due to the difficulties associated with directly analyzing reaction mixtures in the conditions used to prepare many MOF materials, such as hydro- or solvothermal synthesis. The most success to date has been achieved for purely inorganic frameworks such as metal phosphates and silicates, where specific aggregates or secondary building units (SBUs) have been identified during the assembly process.[26] In a recent review, Cheetham and Rao noted that there is no analogous *in situ* characterization of an assembly process for MOFs.[27] Attempts to elucidate pathways for assembly have been through systematic studies of the changes in the structures of the products on varying reaction conditions. For example, a combined powder and single-crystal X-ray diffraction study of a molecular zinc oxalate dimer has shown that it transforms to closely related 1D, 2D, and 3D polymers in distinct stages upon heating.[28] The inference made from this work was that the lower dimensionality polymers act as templates for framework growth. The most direct evidence for the participation of discrete SBUs in the formation of MOFs comes from an EXAFS study by Férey, who identified the presence of a trimeric iron oxide oligomer throughout the formation of the oxycarboxylate $Fe_3O(CH_3OH)_3$-$[O_2C$-$(CH_2)_6$-$CO_2]$·Cl·$(CH_3OH)_6$.[29] The crystal growth of MOF-5 has also recently been monitored by light scattering,[30] and the composition of the gaseous species emitted during framework synthesis have been analyzed, giving insights into the fundamental reactions taking place.[31] Our present system proved to be amenable to analysis by electrospray ionization mass spectrometry (ESI−MS).[32] This very mild ionization technique has been widely used for the determination of solution species in self-assembled capsule chemistry[33] and also for some

(10) Palomino, G. T.; Carayol, M. R. L.; Arean, C. O. *J. Mater. Chem.* **2006**, *16*, 2884.
(11) (a) Henderson, K. W.; Kerr, W. J. *Chem.−Eur. J.* **2001**, *7*, 3430. (b) He, X.; Noll, B. C.; Beatty, A.; Mulvey, R. E.; Henderson, K. W. *J. Am. Chem. Soc.* **2004**, *126*, 7444. (c) He, X. Y.; Allan, J. F.; Noll, B. C.; Kennedy, A. R.; Henderson, K. W. *J. Am. Chem. Soc.* **2005**, *127*, 6920. (d) Hull, K. L.; Noll, B. C.; Henderson, K. W. *Organometallics* **2006**, *25*, 4072. (e) Wendell, L. T.; Bender, J.; He, X.; Noll, B. C.; Henderson, K. W. *Organometallics* **2006**, *25*, 4953. (f) He, X.; Morris, J. J.; Noll, B. C.; Brown, S. N.; Henderson, K. W. *J. Am. Chem. Soc.* **2006**, *128*, 13599.
(12) (a) Rood, J. A.; Noll, B. C.; Henderson, K. W. *Inorg. Chem.* **2006**, *45*, 5521. (b) Rood, J. A.; Noll, B. C.; Henderson, K. W. *Main Group Chem.* **2006**, *5*, 21.
(13) (a) Dincă, M.; Long, J. R. *J. Am. Chem. Soc.* **2005**, *127*, 9376. (b) de Lill, D. T.; Bozzuto, D. J.; Cahill, C. L. *Dalton Trans.* **2005**, 2111. (c) Senkovska, I.; Kaskel, S. *Eur. J. Inorg. Chem.* **2006**, 4564. (d) Xiao, D.-R.; Wang, E.-B.; An, H.-Y.; Li, Y.-G.; Su, Z. M.; Sun, C.-Y. *Chem.−Eur. J.* **2006**, *12*, 6528. (e) Davies, R. P.; Less, R. J.; Lickless, P. D.; White, A. J. P. *Dalton Trans.* **2007**, 2528. (f) Volkringer, C.; Loiseau, T.; Férey, G.; Warren, J. E.; Wragg, D. S.; Morris, R. E. *Solid State Sci.* **2007**, *9*, 455.
(14) Abrahams, B. F.; Moylan, M.; Orchard, S. D.; Robson, R. *Angew. Chem., Int. Ed.* **2003**, *42*, 1848.
(15) (a) Vaidhyanathan, R.; Bradshaw, D.; Rebilly, J.-N.; Barrio, J. P.; Gould, J. A.; Berry, N. G.; Rosseinsky, M. J. *Angew. Chem., Int. Ed.* **2006**, *45*, 6495. (b) Anokhina, E. V.; Go, Y. B.; Lee, Y.; Vogt, T.; Jacobson, A. J. *J. Am. Chem. Soc.* **2006**, *128*, 9957.
(16) Thushari, S.; Cha, J. A. K.; Sung, H, H.- Y.; Chui, S. S.-Y; Leung, A. L.-F; Yen, Y.- F.; Williams, I. D. *Chem. Commun.* **2005**, 5515.
(17) Au-Yeung, A. S.-F.; Sung, H, H.- Y.;. Cha, J. A. K.; Siu, A. W.- H.; Chui, S, S.-Y.; Williams, I. D. *Inorg. Chem. Commun.* **2006**, *9*, 507.
(18) (a) Beghidja, A.; Rogez, G.; Rabu, P.; Welter, R.; Drillon, M. *J. Mater. Chem.* **2006**, *16*, 2715. (b) Liu, J.-Q.; Wang, Y.-Y.; Liu, P.; Wu, W.-P.; Wu, Y. P.; Zeng, X.-R.; Zhong, F.; Shi, Q. Z. *Inorg. Chem. Commun.* **2007**, *10*, 343.
(19) Beghidja, A.; Rogez, G.; Rabu, P.; Welter, R.; Drillon, M. *J. Mater. Chem.* **2006**, *16*, 2715.
(20) Song, Y.-S.; Yan, B.; Chen, Z.-X. *J. Solid State Chem.* **2006**, *179*, 4037.
(21) (a) Chen, Z.-F.; Zhang, J.; Xiong, R.-G.; You, X.-Z. *Inorg. Chem. Commun.* **2000**, *3*, 493. (b) Xiong, R.-G.; Zuo, J.-L.; You, X.-Z.; Fun, H.-K.; Raj, S. S. S. *New J. Chem.* **1999**, *23*, 1051. (c) Dybstev, D. N.; Nuzhdin, A.; Fedin, V.; Kim, K. *Angew. Chem., Int. Ed.* **2006**, *45*, 916.
(22) (a) Wu, C.-D.; Lin, W. *Dalton Trans.* **2006**, 4563; (b) Wu, C.-D.; Lin, W. *Chem. Commun.* **2005**, 3673.
(23) (a) Zeng, M.-H.; Wang, B.; Wang, X.-Y.; Zhang, W.-X.; Cheng, X.-M.; Gao, S. *Inorg. Chem.* **2006**, *45*, 7069. (b) Hou, Y.; Yang, M.; Li, G.-H; Feng, S.-H. *Chem. Res. Chinese U.* **2005**, *21*, 406. (c) Thuéry, P. *Eur. J. Inorg. Chem.* **2006**, 3646. (d) Burrows, A. D.; Harrington, R. W.; Mahon, M. F.; Teat, S. J. *Eur. J. Inorg. Chem.* **2006**, 766.
(24) Ramanan, A.; Whittingham, M. S. *Cryst. Growth. Des.* **2006**, *6*, 2419.
(25) (a) Wuest, J. D. *Chem. Commun.* **2005**, 5830. (b) Hosseini, M. W. *Acc. Chem. Res.* **2005**, *38*, 313.
(26) (a) Murugavel, R.; Walawalkar, M. G.; Dan, N.; Roesky, H. W.; Rao, C. N. R. *Acc. Chem. Res.* **2004**, *37*, 763. (b) Férey, G. *J. Solid State Chem.* **2000**, *152*, 37. (c) Norquist, A. J.; O'Hare, D. *J. Am. Chem. Soc.* **2004**, *126*, 6673. (d) Oliver, S.; Kuperman, A.; Ozin, G. A. *Angew. Chem., Int. Ed.* **1998**, *37*, 46. (e) Rao, C. R. N.; Natarajan, S.; Ahoudhury, A.; Neeraj, S.; Ayi, A. A. *Acc. Chem. Res.* **2001**, *34*, 80.
(27) Cheetham, A. K.; Rao, C. N. R.; Feller, R. K. *Chem. Commun.* **2006**, 4780.
(28) Dan. M.; Rao, C. N. R. *Angew. Chem., Int. Ed.* **2006**, *45*, 281.
(29) Surblé, S.; Milange, F.; Serre, C.; Férey, G.; Walton, R. J. *Chem. Commun.* **2006**, 1518.
(30) Hermes, S.; Witte, T.; Hikov, T.; Zacher, D.; Bahnmüller, S.; Langstein, G.; Huber, K.; Fischer, R. A. *J. Am. Chem. Soc.* **2007**, *129*, 5324.
(31) Hausdorf, S.; Baitalow, F.; Seidel, J.; Mertens, F. O. R. L. *J. Phys. Chem. A.* **2007**, *111*, 4259.
(32) Fenn, J. B.; Mann, M.; Meng, C. K.; Wong, S. F.; Whitehouse, C. M. *Science* **1989**, *246*, 64.

precursor solutions that produce coordination polymers.[34] Furthermore, ESI−MS has proved to be a very useful technique in determining the nucleation pathways of zeolitic materials.[35] Herein, we show that ESI−MS is a useful method for identifying the key secondary building units (SBUs) present in metal carboxylate solutions. Such information substantially increases our ability to predict the topologies of the extended networks produced from association of these SBUs.

Results and Discussion

Synthesis and Structural Characterization of 1. Upon optimization of the reaction conditions, high quality, colorless, cubic crystals were deposited from an equimolar mixture of magnesium nitrate and (+)-camphoric acid dissolved in acetonitrile that was maintained at 60 °C for 4 days. Single-crystal X-ray diffraction analysis, in combination with complementary analytical techniques (see later), revealed the formation of the magnesium MOF $[Mg_2(Hcam)_3{\cdot}3H_2O]{\cdot}NO_3{\cdot}MeCN$, **1**. A temperature study on the formation of **1** indicated that it could also be prepared anywhere in the range of 60−120 °C (solvothermal conditions inside a Teflon-lined stainless steel bomb) but the higher temperatures resulted in lower yields and with the formation of smaller crystals. Lowering the temperature below 50 °C led to the sole precipitation of $Mg(NO_3)_3{\cdot}6H_2O$. Therefore, the temperature of crystallization is key to both the synthesis of the MOF and also for the formation of good quality crystals.

Compound **1** crystallizes in the very rare, chiral, cubic space group *I*23 (Tables 1 and 2). Indeed, there are less than 60 reports of *I*23 in the Cambridge Structural Database out of over 400 000 entries.[36] Due to its complexity, discussion of the extended structure of **1** will begin with its simplest repeating building blocks. As shown in Figure 2, the basic structural units within **1** are 3-fold $[Mg_2(Hcam)_3]^+$ paddle-wheels, where a pair of metal centers are bridged in a η^2,μ^2-fashion by three carboxylates (Mg1−O1, 1.982(2); Mg2−O2, 2.050(2) Å). The two metals are octahedrally coordinated to six oxygen centers; however, they are in distinctly different environments. Specifically, in addition to binding to the three bridging carboxylate ligands, Mg2 is η^1-solvated by three protonated carboxylic acids (Mg2−O4 2.113(2) Å). In comparison, Mg1 bonds to three water molecules (Mg1−O5, 2.133(4) Å), as well as the three carboxylates. Both metals are approximately octahedrally coordinated; Mg2 is less distorted from ideal, with O−Mg−O angles ranging between 86.38(14) and 98.61(8)° compared to 78.69(18) and 101.08(10)° for Mg1. The most acute angles for both metals are those between the ligating neutral groups (carboxylic acid or water). Overall, this asymmetrically solvated dimeric unit appears to be a unique structural motif for either molecular or extended carboxylates incorporating any type of metal.[36] Triply carboxylate-bridged magnesium centers have previously been characterized, but these are normally incorporated within

Table 1. Crystallographic Data for Compounds **1** and **2**

	1	**2**
formula	$C_{31}H_{42}Mg_2N_2O_{18}$	$C_{16}H_{30}MgO_8$
fw	788.25	374.71
T, K	100(2) K	100(2) K
crystal system	cubic	orthorhombic
space group	*I*23	$P2_12_12$
a, Å	19.8783(1)	16.0139(3)
b, Å	19.8783(1)	18.4185(4)
c, Å	19.8783(1)	6.3970 (1)
α, deg	90	90
β, deg	90	90
γ, deg	90	90
V, Å^3	7854.84(4)	1886.81(6)
Z	8	4
D, Mg/ m^3	1.159	1.319
μ, (Cu Kα), mm^{-1}	1.070	1.166
cryst size, mm	0.42 × 0.41 × 0.34	0.48 × 0.12 × 0.08
T_{max} and T_{min}	0.66 and 0.57	0.92 and 0.87
$\theta_{min}-\theta_{max}$, deg	3.14−67.80	3.66−65.53
reflections collected	14472	9680
ind reflections	2319	2952
R(int)	0.0250	0.0263
obs. refl., [$I > 2\sigma(I)$]	2262	2780
*R*1,[a] *wR*2[b], [$I > 2\sigma(I)$]	0.0571, 0.1686	0.0301, 0.0716
*R*1, *wR*2 (all data)	0.0578, 0.1694	0.0332, 0.0721
goodness-of-fit[c] on F^2	1.054	1.447

[a] $R1 = \sum ||F_o| - |F_c|| / \sum |F_o|$. [b] $wR2 = \{\sum [w(F_o^2 - F_c^2)^2] / \sum [w(F_o^2)^2]\}^{1/2}$; $w^{-1} = [\sigma^2(F_o^2) + (0.1325P)^2 + 9.6648P]$; $P = (F_o^2 + 2F_c^2)/3$. [c] $GOF = S = \{\sum [w(F_o^2 - F_c^2)^2] / (n - p)\}^{1/2}$; n = number of reflections, p = number of parameters.

Table 2. Selected Bond Lengths [Å] and Angles [deg] for **1**[a]

Bond Lengths [Å]			
Mg(1)−O(1)	1.982(2)	Mg(1)−O(5)	2.134(4)
Mg(2)−O(2)	2.050(2)	Mg(2)−O(4)	2.112(2)
O(1)−C(1)	1.235(4)	O(2)−C(1)	1.269(4)
O(3)−C(10)	1.309(4)	O(4)−C(10)	1.216(4)

Bond Angles [deg]			
O(1)#1−Mg(1)−O(1)	101.08(10)	O(1)#1−Mg(1)−O(5)	91.7(2)
O(1)−Mg(1)−O(5)	163.54(17)	O(1)−Mg(1)−O(5)#1	86.38(14)
O(5)−Mg(1)−O(5)#1	78.69(18)	O(2)−Mg(2)−O(2)#1	98.61(8)
O(2)−Mg(2)−O(4)#3	85.98(8)	O(2)−Mg(2)−O(4)#4	88.41(8)
O(2)−Mg(2)−O(4)#5	170.89(10)	C(1)−O(1)−Mg(1)	143.6(2)
C(1)−O(2)−Mg(2)	141.52(19)	C(10)−O(4)−Mg(2)#6	135.2(2)

[a] Symmetry transformations used to generate equivalent atoms: #1 *y*−1,*z*+1,*x*; #2 *z*,*x*+1,*y*−1; #3 −*z*+1/2,−*x*+3/2,*y*−1/2; #4 *y*−1/2,−*z*+3/2,−*x*+1/2; #5 −*x*+1/2,*y*+1/2,−*z*+1/2; #6 −*x*+1/2,*y*−1/2,−*z*+1/2.

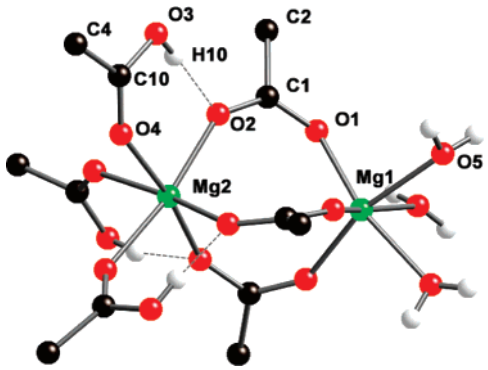

Figure 2. Three-fold dimetallic paddle-wheel component of **1** showing the three terminally bound water molecules, the three bridging carboxylates, and the three ligating carboxylic acids that are involved in hydrogen bonding (only the methine carbons of the acids are shown for clarity).

(33) (a) Andersen, U. N.; Seeber, G.; Fiedler, D.; Raymond, K. N. *J. Am. Soc. Mass. Spectrom.* **2006**, *17*, 292. (b) Konig, S.; Bruckner, C.; Raymond, K. N.; Leary, J. A. *J. Am. Soc. Mass. Spectrom.* **1998**, *9*, 1099. (c) Yeh, R. M.; Xu, J.; Seeber, G.; Raymond, K. N. *Inorg. Chem.* **2005**, *44*, 6228. (d) Pluth, M. D.; Raymond, K. N. *Chem. Soc. Rev.* **2007**, *36*, 161. (e) Kumazawa, K.; Yoshizawa, M.; Liu, H.-B.; Kamikawa, Y.; Moriyama, M.; Kato, T.; Fujita, M. *Chem.−Eur. J.* **2005**, *11*, 2519. (f) Ellis, W. W.; Schmitz, M.; Atta, A.; Stang, P. J. *Inorg. Chem.* **2000**, *39*, 2547.
(34) (a) Hirsch, K. A.; Wilson, S. R.; Moore, J. S. *J. Am. Chem. Soc.* **1997**, *119*, 10401. (b) Johannson, F. B.; Bond, A. D.; McKenzie, C. J. *Inorg. Chem.* **2007**, *46*, 2224.
(35) (a) Pelster, S. A.; Kalamajka, R.; Schrader, W.; Schüth, F. *Angew. Chem., Int. Ed.* **2007**, *119*, 2349. (b) Bussian, P.; Sobott, F.; Brutschy, B.; Schrader, W.; Schüth, F. *Angew. Chem., Int. Ed.* **2001**, *39*, 3901. (c) Pelster, S. A.; Schrader, W.; Schüth, F. *J. Am. Chem. Soc.* **2006**, *128*, 4310.
(36) Allen, F. H. *Acta Crystallogr.* **2002**, *B58*, 380.

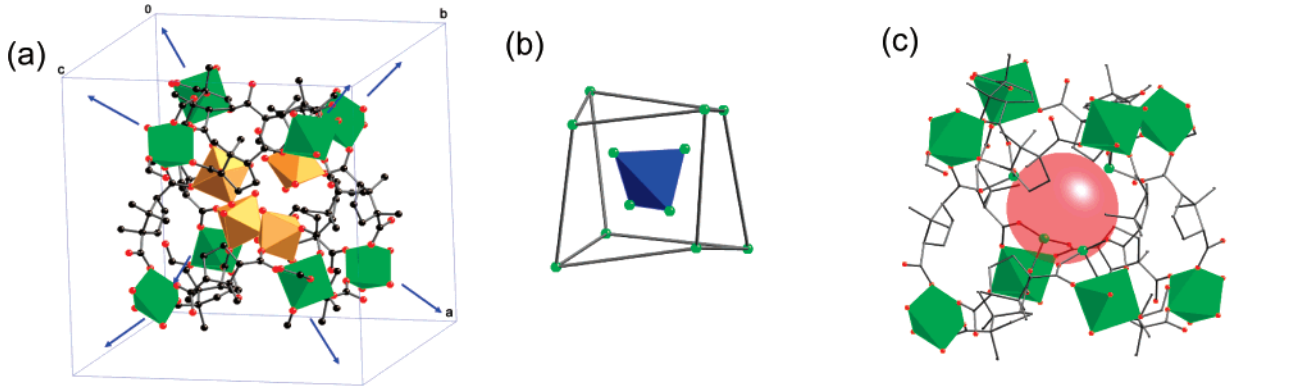

Figure 3. (a) Mg_{12} cage within the unit cell of **1**, illustrating the relative positions of the four water-solvated core metals (brown octahedra) and the eight outer metals (green octahedra) that act as points of framework extension. (b) View of the Mg_4 core as a blue tetrahedron encapsulated within the distorted Mg_8 cubane. (c) Mg_{12} cage with encapsulated water molecules removed. The red sphere shows the available space within the chiral cavity.

Mg_3 trimeric aggregates.[37] The only other example of a dimeric magnesium 3-fold paddle-wheel that has been structurally characterized is the complex $[Mg_2(O_2CNCy_2)_4 \cdot (HMPA)]$.[38] This species crystallizes with the carbamate groups adopting three different binding modes: two $\eta^2,\mu;^2$ one η^3,μ^2; and one simply $\eta^2,\mu,^1$ which contrasts with the symmetrical η^2,μ^2 binding of the carboxylates in **1**.

In **1**, the protonated nature of the carboxylic acid unit at C10 is supported by location of the proton H10 bonded to O3 in the difference Fourier map from the X-ray structure. Also, C10−O3 is almost 0.1 Å longer than C10−O4, as would be expected for localized single and double C−O bonds within a carboxylic acid (1.309(4) and 1.216(4) Å, respectively).[39] A potentially important feature for the supramolecular assembly of **1** is the formation of a hydrogen bond between H10 of the acid and O2 of the bridging carboxylate. The H10−O2 distance is 1.758(8) Å, the O2−O3 separation is 2.571(6) Å, and the O2−H10-O3 angle is 163.71(8)°, which in combination suggests a relatively strong hydrogen bonding interaction.[40]

The next repeating units found in the extended structure are entirely novel $Mg_{12}(Hcam)_{12} \cdot 12H_2O$ cages, produced by association of the dimetallic units through the neutral bridging carbonyl groups of the acids (Figure 3a). The Mg_{12} cages can be described by the location of the metal centers as Mg_4 tetrahedra encapsulated within Mg_8 cubes (Figure 3b). Eight of the metals define a distorted cube, with all sides being 10.0800(4) Å and the internal angles being either 75.75(2) or 102.62(2)°. At the center of each Mg_8 cube is a perfect Mg_4 tetrahedron, with sides of 5.754(3) Å and internal angles of 60°. Each of the four metals of the tetrahedra are solvated by three terminal water molecules, and they are oriented such that all 12 water molecules are directed toward the center of the cage. Thus, the extended structure of **1** has large, isolated cavities with an approximate volume of 1058 $Å^3$ (Figure 3c).[41] This arrangement of scattered "dots" or "0D cavities" is a highly unusual form of a porous solid, as recently defined by Kitagawa,[42] where 1D channels, 2D layers, or 3D intersecting channels are normally encountered.[43] Presumably, the major source of the water is from the hydrated nitrate starting material. There appears to be significant hydrogen bonding between the 12 water molecules within the 0D cavity, which possibly aids in the stabilizing the unusual structure. The presence of hydrogen bonding may also explain the rather long Mg1−O5 distances of 2.134(4) Å, compared with the mean value of 2.07 Å found for water bound to an octahedrally coordinated magnesium center.[36]

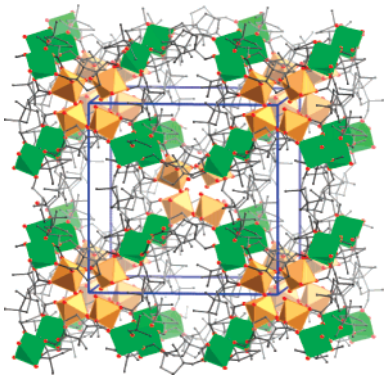

Figure 4. View of the eight Mg_{12} cages centered at the corners of the unit cell to give the **bcu** network.

Finally, the extended 3D structure of **1** is a rare example of a body-centered cubic (**bcu**) MOF.[44] The eight metal centers on the corners of the Mg_8 cube act as points of network extension and are incorporated as vertices of neighboring cubes (Figure 4). Therefore, the centroid of the Mg_{12} cage can be considered as an eight-connected node to give a 3D network with the Schläfli symbol $4^{24}.6^4$.[45] MOFs derived from nodes with greater than six points of extension, high connectivity networks, are a topic of current interest.[46] Schröder and Champness prepared the first eight-connected **bcu** nets in 2001

(37) (a) Ruben, M.; Walther, D.; Knake, R.; Goris, H.; Beckert, R. *Eur. J. Inorg. Chem.* **2000**, 1055. (b) Coker, E. N.; Boyle, T. J.; Rodriguez, M. A.; Alam, T. M. *Polyhedron*, **2004**, *23*, 1739. (c) Yang, K.-C.; Chang, C.-C.; Yeh, C.-S.; Lee, S.-M. P. *Organometallics* **2001**, *20*, 126.
(38) Tang, Y.; Zakharov, L. N.; Rheingold, A. L.; Kemp, R. A. *Organometallics* **2004**, *23*, 4788.
(39) Allen, F. H.; Kennard, O.; Watson, D. G.; Brammer, L.; Orpen, A. G. *J. Chem. Soc. Perkin Trans.* **1987**, *2*, S1.
(40) Steed, J. W.; Atwood, J. L. *Supramolecular Chemistry*; Wiley: New York, 2000.
(41) Spek, A. L. *PLATON, A Multipurpose Crystallographic Tool*; Utrecht University: Utrecht, The Netherlands, 2001.
(42) Kitagawa, S.; Kitaura, R.; Noro, S. *Angew. Chem., Int. Ed.* **2004**, *43*, 2334.
(43) Batten, S. R.; Hoskins, B. F.; Robson, R. *J. Am. Chem. Soc.* **1995**, *117*, 5385.
(44) The bolded net abbreviation is derived from the RCSR database. (a) O'Keeffe, M.; Yaghi, O. M.; Ramsden, S. *Reticular Chemistry Structure Resource*; Arizona State University: Tempe, AZ, 2007; database available at http://rcsr.anu.edu.au. (b) Delgado-Friedrichs, O.; O'Keeffe, M.; Yaghi, O. M. *Phys. Chem. Chem. Phys.* **2007**, *9*, 1035.
(45) For a review on network nomenclature see: Delgado-Friedrichs, O.; O'Keeffe, M. *J. Solid State Chem.* **2005**, *178*, 2480.
(46) Hill, R. J.; Long, D.-L.; Champness, N. R.; Hubberstey, P. Schröder, M. *Acc. Chem. Res.* **2005**, *38*, 337.

through the use of large lanthanide metal ions in conjunction with the narrow linker 4,4′-bipyridine-*N*,*N*′-dioxide.[47] More recently, Zhu and Qiu reported the **bcu** MOF $[Cd_{11}(\mu_4\text{-}HCO_2)_6(bpdc)_9]$, ($H_2$bpdc = 4,4′-biphenyldicarboxylic acid), which is constructed from Cd_{11} cages.[48] Compound **1** differs from the previously characterized examples of **bcu** MOFs as it is composed of vertex-shared cages, as opposed to isolated metals or cages which are connected by bridging ligands. It is also interesting to note that the body-centered cubic topology of the network is reflected within the crystallographic cubic space group *I*23.

Physical Properties of 1. The framework is positively charged and the material is rendered neutral by nitrate molecules that occupy the interstitial spaces between the Mg_{12} cages. These spaces are also likely filled by disordered acetonitrile molecules to give the overall formula of $[Mg_2(Hcam)_3{\cdot}3H_2O]{\cdot}NO_3{\cdot}$MeCN. The presence of both nitrate and acetonitrile is supported by elemental analyses, IR, ESI−MS, and NMR data (see the experimental section and the Supporting Information). In addition, thermogravimetric analysis (TGA) of **1** run under an N_2 atmosphere indicated a weight loss of 9.8% between 25 and 175 °C, partially accounting for the theoretical loss of 12.1% due to the complete removal of the water and acetonitrile. After this initial loss, a second weight loss of 32.2% occurs sharply between 175 and 225 °C (42% total loss), most likely indicating the formation of a new phase. This new phase remains stable until total decomposition occurs at 495 °C. A crystalline sample of **1** was heated under dynamic vacuum ($\sim 10^{-2}$ Torr) at 170 °C for 72 h to determine if the structure of the network was retained on removal of the solvents. During this time, the crystals transformed to a powder. Subsequent powder X-ray diffraction (PXRD) analyses illustrated that the structure of **1** was not retained upon desolvation but a new crystalline phase was produced (see Supporting Information). This result supports the assessment that the structure of **1** contains isolated water-filled cavities rather than porous channels and that destruction of the extended structure is required to remove the encapsulated water.

The chirality of the camphorate ligand is clearly retained in **1**, as determined by crystallography. Polarimetry was used to independently verify that the bulk sample of **1** maintained its chirality. This was achieved by comparing the optical rotations of equimolar solutions (with respect to ligand) of compound **1** and pure (+)-camphoric acid in NaOH. Thus, camphoric acid is a reliable and robust chiral linker molecule for the preparation of MOF materials.

Additive Studies. Although the structure of **1** does not possess channels suitable for molecular exchange, it does contain large chiral cavities that are filled with water (Figure 3c). The possibility of selectively capturing alternative small molecules or even preferentially separating enantiomeric mixtures within this cavity during network formation was investigated. A series of reactions similar to the preparation of **1** were conducted with the addition of five molar equivalents of various additives, including small amines, alcohols and glymes (see the experimental section). Thus far this strategy has mainly resulted in either the preparation of **1** or the formation of noncrystalline materials. The additive reaction involving 1,3-propanediol was particularly interesting as it produced crystals that could be analyzed by crystallography. In turn, the structure of $[Mg(cam)\{HO(CH_2)_3OH\}_2]$, **2**, was determined by X-ray diffraction (Tables 1 and 3, Figure 5). The structure of **2** is composed of 1D chiral chains, where the camphorate ligands bridge between diol-chelated metal centers. In contrast to **1**, the metals now bind to two carboxylates in an η^1,μ^1-fashion (Mg−O = 2.0564(14) and 2.0648(15) Å) and their octahedral coordination spheres are completed by bonding to two chelating 1,3-propanediol molecules (range Mg−O = 2.0532(15)−2.0952(16) Å). Similar 1D chains have previously been characterized for magnesium salts of dicarboxylic acids.[49] As with **1**, the chirality of the camphorate is retained and the ligands are oriented in an anti manner with respect to each other along the chain.

Table 3. Selected Bond Lengths [Å] and Angles [deg] for **2**[a]

Bond Lengths [Å]			
Mg(1)−O(5)	2.0530(14)	Mg(1)−O(1)	2.0560(13)
Mg(1)−O(2)	2.0655(14)	Mg(1)−O(3)	2.0693(14)
Mg(1)−O(6)	2.0784(14)	Mg(1)−O(4)	2.0944(15)
O(1)−C(1)	1.255(2)	O(2)−C(4)	1.255(2)
O(3)−C(16)	1.424(2)	O(8)−C(4)	1.272(2)
O(4)−C(14)	1.432(3)	O(6)−C(13)	1.434(2)
O(5)−C(11)	1.422(2)	O(7)−C(1)	1.269(2)
Bond Angles [deg]			
O(5)−Mg(1)−O(1)	89.06(6)	O(5)−Mg(1)−O(2)	90.90(6)
O(1)−Mg(1)−O(2)	177.15(6)	O(5)−Mg(1)−O(3)	178.17(6)
O(1)−Mg(1)−O(3)	89.30(6)	O(2)−Mg(1)−O(3)	90.78(6)
O(5)−Mg(1)−O(6)	87.52(6)	O(1)−Mg(1)−O(6)	89.46(6)
O(2)−Mg(1)−O(6)	93.38(6)	O(3)−Mg(1)−O(6)	91.64(6)
O(5)−Mg(1)−O(4)	92.98(6)	O(1)−Mg(1)−O(4)	89.56(6)
O(2)−Mg(1)−O(4)	87.60(6)	O(3)−Mg(1)−O(4)	87.83(6)
O(6)−Mg(1)−O(4)	178.89(6)	C(4)−O(2)−Mg(1)	130.63(12)
C(1)−O(1)−Mg(1)	133.80(12)	C(14)−O(4)−Mg(1)	122.58(13)
C(16)−O(3)−Mg(1)	122.31(12)	C(11)−O(5)−Mg(1)	123.08(12)
C(13)−O(6)−Mg(1)	121.04(13)		

[a] Symmetry transformations used to generate equivalent atoms: #1 $-x+3/2,y-1/2,-z+1$; #2 $-x+3/2,y+1/2,-z+1$.

Clearly, the addition of the diol results in a very different outcome in the solid state, with isolated metals replacing the dimetallic paddle-wheels seen in **2**. Presumably, this is a consequence of the formation of new solution species on addition of the additive. This speculation led us to consider directly analyzing the complexes present in the precursors solutions during the formation of the networks **1** and **2**.

Mass Spectrometric Studies. We were interested in gaining more specific information on the identity of the solution species present during the crystal growths of **1** and **2**. We opted to investigate the use of ESI−MS, as ESI is a very mild ionization technique which minimizes perturbations of the species present in solution. Also, our system appeared to be particularly suitable for analysis by this method as all of the starting materials are entirely soluble in acetonitrile (an excellent solvent for ESI−MS), and furthermore the postulated 3-fold $[Mg_2(Hcam)_3]^+$ paddle-wheel SBUs in **1** carry single positive charges.[50]

(47) Long, D.-L.; Blake, A. J.; Champness, N. R.; Wilson, C.; Schröder, M. *Angew. Chem., Int. Ed.* **2001**, *40*, 2443.
(48) Fang, Q.-R.; Zhu, G.-S.; Jin, Z.; Xue, M,; Wei, X.; Wang, D.-J.; Qiu, S.-L. *Angew. Chem., Int. Ed.* **2006**, *45*, 6126.
(49) (a) Ptasiewicz-Bak, H.; Leciejewicz, J. *Pol. J. Chem.* **1997**, *71*, 493. (b) Baier, J.; Thewalt, U.; *Z. Anorg. Allg. Chem.* **2002**, *628*, 1890. (c) Ojala, W. H.; Khankari, R. K.; Grant, D. J. W.; Gleason, W. B. *J. Chem. Cryst.* **1996**, *26*, 167. (d) Baier, J.; Thewalt, U. *Z. Anorg. Allg. Chem.* **2002**, *628*, 315. (e) Fleck, M.; Tillmanns, E.; Haussuhl, S. *Z. Kristallogr. New Cryst. Struct.* **2000**, *215*, 107.
(50) (a) Stone, J. A.; Su, T.; Vukomanovic, D. *Int. J. Mass Spectrom.* **2002**, *216*, 219. (b) Ouyang, S.; Vairavamurthy, M. A. *Anal. Chim. Acta* **2000**, *422*, 101.

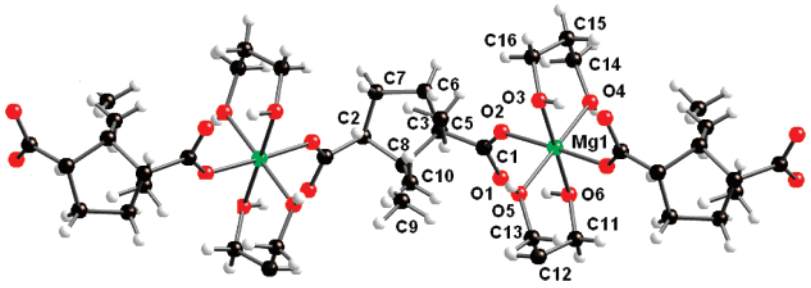

Figure 5. Section of the extended 1D polymeric structure of **2**, with hydrogens removed for clarity.

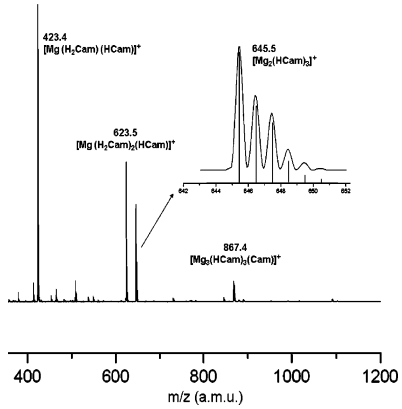

Figure 6. ESI−MS (positive ion mode) of a mixture of $Mg(NO_3)_2 \cdot 6H_2O$ and (+)-camphoric acid in acetonitrile using a cone voltage of 25 V. (Inset) Comparison of the experimental signal for the 3-fold paddle-wheel with the calculated isotopic distribution.

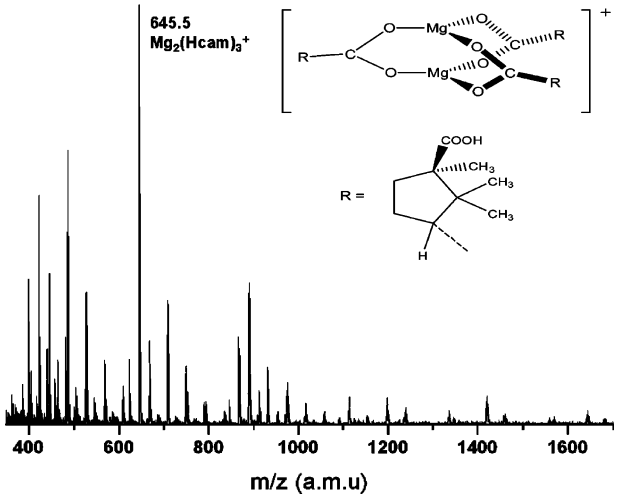

Figure 7. ESI−MS (positive ion mode) of a mixture of $Mg(NO_3)_2 \cdot 6H_2O$ and (+)-camphoric acid in acetonitrile using a cone voltage of 200 V.

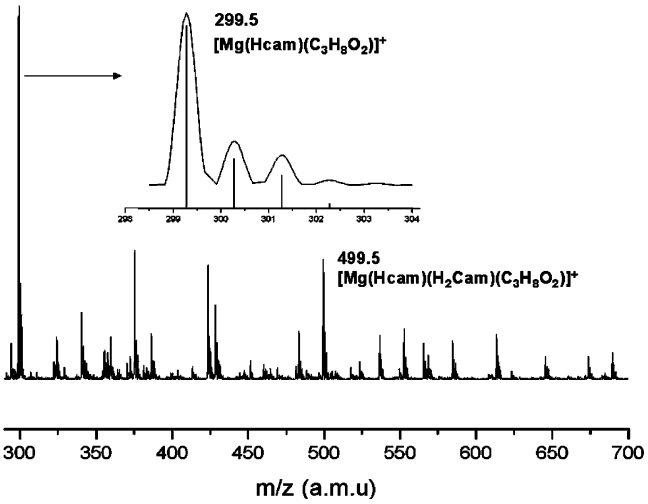

Figure 8. ESI−MS (positive ion mode) of a mixture of $Mg(NO_3)_2 \cdot 6H_2O$, (+)-camphoric acid and 1,3-propanediol in acetonitrile using a cone voltage of 25 V. (Inset) Comparison of the experimental and theoretical isotopic distributions for the most abundant ion.

Samples were prepared under various synthetic conditions, and their mass spectra were recorded. Initial experiments used samples that were prepared in an identical manner to those used for the crystallization of **1** (approximately 50 mmol/L in metal). Upon dissolution at ambient temperature, the solutions were then immediately analyzed via direct infusion at a 10 μL/min flow rate. Another set of samples were prepared where the reaction mixtures were maintained at 60 °C for several days to mimic the crystallization conditions. Finally, a dilution study was undertaken where 5 mmol/L and 50 μmol/L samples were analyzed. In all cases, the mass spectra obtained were very similar, with the major species present being consistent independent of the sample preparation. However, the ion source cone voltage used during the experiment proved to be critical in determining the distribution and identity of the species present. The mass spectra with the least number of different ions were obtained at low to moderate cone voltages of 15−75 V. A typical mass spectrum recorded at a cone voltage of 25 V is shown in Figure 6, with the major species present highlighted. Under these conditions, the two most abundant ions are the monomeric species $[Mg(H_2cam)(Hcam)]^+$ and $[Mg(H_2cam)_2(Hcam)]^+$ with *m*/*z* values of 423 and 623, respectively. However, the most revealing signal appears at *m*/*z* 645, which corresponds with the expected 3-fold $[Mg_2(Hcam)_3]^+$ paddle-wheel SBU. The inset in Figure 6 shows the excellent agreement between the experimental and calculated fit for the isotopic distribution pattern for this ion. Isomers of $[Mg_2(Hcam)_3]^+$ would also give the same data. Specifically, the ion $[Mg_2(H_2cam)_2(Hcam)(cam)]^+$ would appear at the same *m*/*z* value and with the same isotopic distribution. Furthermore, the heavier ions in the spectra at *m*/*z* 867 and also at 1089 are consistent with neutral salt, [Mg(cam)], addition products.[50] Nevertheless, systematically increasing the cone voltage was accompanied by an increase in the relative intensity of the *m*/*z* 645 signal, such that at 200 V it is the most abundant ion (Figure 7). At these higher voltages, new ions begin to appear as a result of fragmentation. Also, many of the heavier ions appear to be neutral [Mg(cam)] salt addition products of nitrate-containing ions (see Supporting Information). Further analysis of the *m*/*z* 645 ion by precursor ion MS−MS indicated that it does not have a heavier parent ion. In combination, these data suggest that the *m*/*z* 645 is a particularly stable ion and are consistent

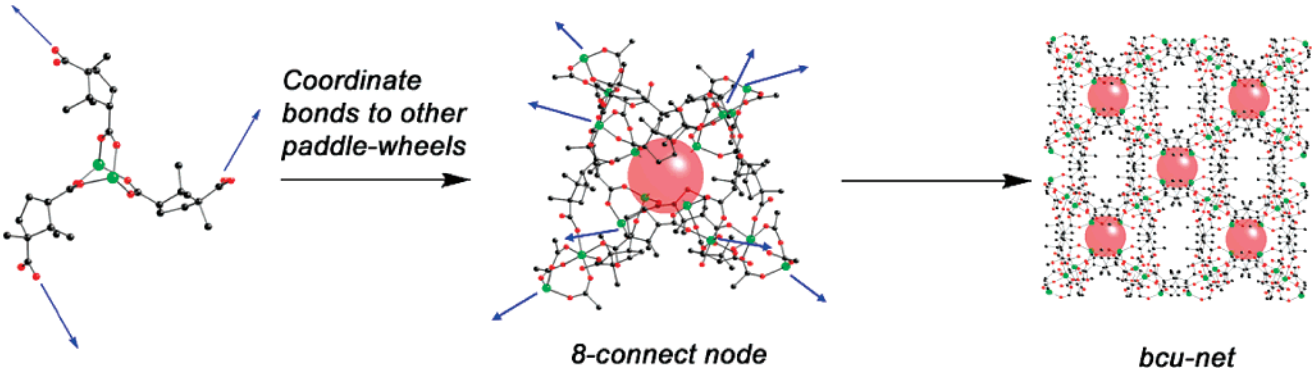

Figure 9. Schematic view of the assembly of the extended **bcu** network of **1** via association of the 3-fold paddle-wheels. The blue arrows indicated the direction of polymer extension.

with this aggregate being present in solution during crystal growth. Product ion MS/MS spectra collected under single collision conditions show that high collision energies are required to produce fragment ions. It is therefore reasonable to conclude that this ion is indeed the 3-fold $[Mg_2(Hcam)_3]^+$ paddle-wheel SBU found within the solid-state structure of **1**.

Next, the consequences of adding 1,3-propanediol to the solutions were investigated. A sample was run under identical conditions to those used for the sample discussed previously to produce Figure 6. As can be seen in Figure 8, addition of the diol results in a significantly more complex spectrum. The signals present in Figure 6 are retained but a number of new species also appear. In particular, the most abundant ion is clearly the *m*/*z* 299 signal, corresponding to the diol complex $[Mg(Hcam)(C_3H_8O_2)]^+$. This supports the assertion that addition of the diol results in the formation of new chelated solution species. In turn, this leads to the preferential crystallization of **2** instead of **1** under these circumstances.

In combination, these data support the assertion that the solid-state assembly process for **1** involves the participation of soluble $[Mg_2(Hcam)_3]^+$ SBUs. These are very likely solvated by either water and/or acetonitrile in solution, which are lost upon ionization. Identification of the $[Mg_2(Hcam)_3]^+$ SBU in solution allows us to speculate on their role in the assembly of **1**. A reasonable model is that the stable paddle-wheel cations associate using neutral carboxylates as linkers. This association is promoted by the formation of strong hydrogen bonding interactions between the protonated acids and the bridging carboxylates. At this stage, there are multiple possible coordination modes between the SBUs. However, each metal is very likely to be hexacoordinated, requiring solvation by three external donors in addition to the carboxylates. The unsymmetrical solvation of the SBUs found in **1** may be driven by the formation of hydrogen bonds between the water molecules of neighboring dimers. In turn, this leads to the creation of the water-filled 0D cavities. Indeed, it is notable that water preferentially solvates one of the metal centers in **1** despite the presence of acetonitrile as bulk solvent media. Examination of the 0D cavities shows that there is insufficient space available for 12 aceotnitriles that would be required to maintain the hexacoordination at the metal centers. Finally, the second metal of the SBU achieves hexacoordination through binding to three carbonyl groups that go on to form the extended **bcu** network (Figure 9).

Conclusions

In summary, MOF **1** is notable on several fronts: (1) it is composed of novel, unsymmetrically solvated $[Mg_2(Hcam)_3 \cdot 3H_2O]^+$ SBU paddle-wheels; (2) association of these SBUs creates unique Mg_{12} cages; (3) each cage has 12 water molecules at its core, forming a 0D cavity; (4) the Mg_{12} cages are fused to eight other cages to form an unusual example of a body-centered cubic MOF; and (5) the chirality of the (+)-camphoric acid is retained, leading to crystallization in the very rare chiral, cubic space group *I*23. Mass spectrometry studies of the precursor acetonitrile solutions of both **1** and the diol solvate **2** show that this technique is useful in the identification of stable SBUs prior to crystal growth. Indeed, the characterization of the stable paddle-wheel $[Mg_2(Hcam)_3]^+$ cation in solution lends strong support to the assertion that it is the true building block for network assembly. We are presently extending the ESI−MS studies to other network syntheses in an effort to test the scope of this technique to aid in rationalizing the mechanisms of MOF formation.

Experimental Section

General. Acetonitrile was dried by distillation over calcium hydride and stored over 4 Å molecular sieves prior to use. The metal nitrate $Mg(NO_3)_2 \cdot 6H_2O$ and 1,3-propanediol were purchased from Aldrich and used as received. D_2O was purchased from Cambridge Isotope Laboratories and was used for the ^1H NMR spectroscopic studies. ^1H NMR spectra were recorded on a Varian-300 spectrometer at 293 K and were referenced internally to the residual signals of the deuterated solvent. FT-IR spectra were obtained either as Nujol mulls or as KBr pellets on a Nicolet Nexus 870 FT-IR spectrometer in the range of 4000−500 cm^{-1}. Thermogravimetric analyses were performed on a TA instruments Hi-Res Modulated TGA 2950 thermogravimetric analyzer at the rate of 10 °C/min under N_2. Mass spectra were recorded on a Micromass Quatro triple LC quadrupole mass spectrometer. Elemental analyses were performed by Midwest Microlab, Indianapolis, IN.

X-Ray Crystallography. Powder XRD patterns were obtained on a Bruker Smart Apex diffractometer with Cu Kα radiation. The sample was mounted in a capillary. Data were collected by the 2D Apex detector fixed at 100 mm, $2\theta = 20°$, $\omega = 0°$, $\phi = 0°$ for 10 min.

Single crystals were examined under Infineum V8512 oil. The datum crystal was affixed to either a thin glass fiber atop a tapered copper mounting pin or Mitegen mounting loop and transferred to the 100 K nitrogen stream of a Bruker APEX diffractometer equipped with an Oxford Cryosystems 700 series low-temperature apparatus. Cell parameters were determined using reflections harvested from three sets of 36 0.5° ϕ scans. The orientation matrix derived from this was

transferred to COSMO[51] to determine the optimum data collection strategy requiring a minimum of 4-fold redundancy. Cell parameters were refined using reflections harvested from the data collection with $I \geq 10\sigma(I)$. All data were corrected for Lorentz and polarization effects, and runs were scaled using SADABS.[52]

The structures were solved from partial datasets using the Autostructure option in APEX 2.[51] This option employs an iterative application of the direct methods, Patterson synthesis, and dual-space routines of SHELXTL[53] followed by several iterative cycles of least-squares refinement. Hydrogen H10 in **1** was initially located on the difference map and was subsequently modeled similar to the remaining hydrogens, which were placed at calculated geometries and allowed to ride on the position of the parent atom. Hydrogen thermal parameters were set to 1.2× the equivalent isotropic U of the parent atom, 1.5× for methyl hydrogens.

Synthesis of $[Mg_2(Hcam)_3 \cdot 3H_2O] \cdot NO_3 \cdot MeCN$, 1. A mixture of 5 mL of MeCN, 50 mg of (+)-camphoric acid (0.25 mmol), and 65 mg of $Mg(NO_3)_2 \cdot 6H_2O$ (0.25 mmol) was placed in a 20 mL scintillation vial. The vial was capped and immersed in a silicon oil bath, which was kept at a constant temperature of 60 °C for 4 days. During this period high-quality, colorless, cubic crystals of **1** were deposited, 28 mg (88.9%). The crystals were isolated by suction filtration, washed with acetonitrile (3 × 1 mL), and allowed to dry in air. Anal. calcd for **1** (%): C, 47.80; H, 6.72; N, 3.49; Found (%): C, 48.24; H, 6.50, N 3.01. IR (KBr, υ/cm^{-1}): 3383m, 2291w, 1681m, 1601s, 1404m, 1395w, 1366s, 1169w, 1129w, 1088w, 818w, 754w, 722w. ^{1}H NMR (300mHz, D_2O): δ2.81 (t, 1H), δ2.23 (s, 0.7H) δ2.15 (dq, 2H), δ1.70 (dq, 2H), δ1.20 (d, 6H), δ0.82 (s, 3H). PXRD studies also confirmed the bulk homogenaity of the sample.

General Procedure for the Additive Studies. The reaction mixtures were prepared as described for **1** with the addition of five molar equivalents of an additive (methanol, *s*-butanol, 1,2-propanediol, 1,3-propanediol, 1,3-butanediol, ethylene diamine, *N*,*N*,*N*′,*N*′-tetramethyl-ethylene diamine, glyme, diglyme, and tetraglyme). In all cases, with the exception of the 1,3-propanediol, the reactions either resulted in either precipitation of **1** or formation of noncrystalline solids that were not analyzed further.

$[Mg(cam)\{HO(CH_2)_3OH\}_2]$, 2. Yield: 29 mg (30.9%). IR (Nujol mull, υ/cm^{-1}): 3381s, 2285w, 1682m, 1601m, 1567m, 1455m, 1395w, 1374s, 1285w, 1061s, 982w, 924w, 779w, 740w. ^{1}H NMR (300mHz, D_2O): δ3.683 (t, 2H). δ2.68 (t, 1H), δ2.25(dq, 2H), δ1.792 (s, 2H). δ1.70 (dq, 2H), δ1.20 (d, 6H), δ0.772 (s, 3H).

Acknowledgment. We gratefully acknowledge Petroleum Research Fund (41716-AC3) and the National Science Foundation for instrumentation support (CHE-0443233). We also thank the Center for Environmental Science and Technology at Notre Dame for the use of the Micromass Quatro-LC and Professor Paul McGinn for the TGA studies.

Supporting Information Available: Crystallographic data for **1** and **2** in CIF format; NMR, IR, PXRD, ESI−MS, and TGA data; ORTEP pictures of **1** and **2**. This material is available free of charge via the Internet at http://pubs.acs.org.

JA074558J

(51) *APEX2 and COSMO*; Bruker-Nonius AXS: Madison, WI, 1005.
(52) Sheldrick, G. M. University of Göttingen: Germany, 2004.
(53) Sheldrick, G. M. *SHELXTL*; Bruker-Nonius AXS: Madison, WI, 2004.